Video-LLaVA: Learning United Visual Representation by Alignment Before Projection

Anonymous ACL submission

Abstract

The Large Vision-Language Model (LVLM) has enhanced the performance of various downstream tasks in visual-language understanding. Most existing approaches encode images and videos into separate feature spaces, which are then fed as inputs to large language models. However, due to the lack of unified tokenization for images and videos, namely misalignment before projection, it becomes challenging for a Large Language Model (LLM) to learn multi-modal interactions from several poor projection layers. In this work, we unify visual representation into the language feature space to advance the foundational LLM towards a unified LVLM. As a result, we establish a simple but robust LVLM baseline, **Video-LLaVA**, which learns from a mixed dataset of images and videos, mutually enhancing each other. Video-LLaVA achieves superior performances on **a broad range of 9 image benchmarks** across 5 image question-answering datasets and 4 image benchmark toolkits. Additionally, our Video-LLaVA also outperforms Video-ChatGPT by **5.8%, 9.9%, 18.6%, and 10.1%** on MSRVTT, MSVD, TGIF, and ActivityNet, respectively. Notably, extensive experiments demonstrate that Video-LLaVA mutually benefits images and videos within a unified visual representation, outperforming models designed specifically for images or videos. We aim for this work to provide modest insights into the multi-modal inputs for the LLM.

1 Introduction

Recently, LLMs have gained rapid popularity in the AI community, such as GPT-3.5, GPT-4 (OpenAI, 2023), PaLM (Bi et al., 2020; Anil et al., 2023), and BLOOM (Scao et al., 2022). They rely on their powerful language comprehension abilities to follow human-provided instructions and provide corresponding responses. Typically, LLMs can only respond within the text input provided by the user, which is insufficient because human

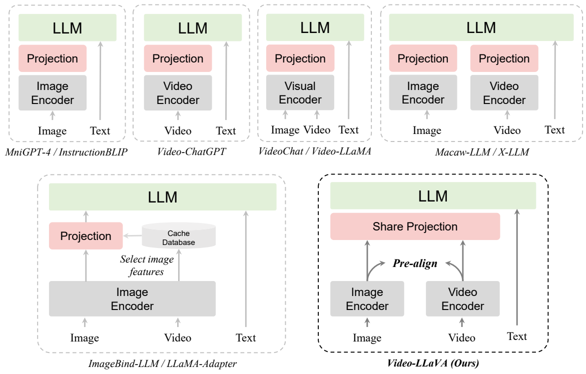

Figure 1: **Comparing Different LVLM Paradigms.** Video-LLaVA aligns images and videos before projection, allowing LLM to learn from a unified visual representation and endowing LLM with the ability to comprehend both images and videos simultaneously.

interaction with the world involves multiple channels, such as visual and textual. To this end, recent works (Ye et al., 2023; Zhu et al., 2023b; Alayrac et al., 2022) have mapped images into text-like tokens, enabling LLMs to emerge with the ability to comprehend images. Despite their effectiveness, empowering LLMs to understand videos is more challenging than image-only comprehension tasks. Nevertheless, recent work (Maaz et al., 2023; Li et al., 2023c; Zhang et al., 2023a) has made initial strides in enabling interactions between video and language.

However, most current LVLMs (Li et al., 2023b; Dai et al., 2023; Luo et al., 2023; Li et al., 2023a) can primarily handle a single visual modality, either image-language or video-language. We compare different LVLM paradigms as shown in Figure 1, where VideoChat (Li et al., 2023c) and Video-LLaMA (Zhang et al., 2023a) utilize a share visual encoder to handle both images and videos. However, due to the inherent differences in the media types of images and videos, it is challenging to learn a unified representation, and the performance falls significantly behind that of the specialized video expert model, Video-ChatGPT. Therefore, X-LLM (Chen et al., 2023) and Macaw-LLM (Lyu et al., 2023) allocate a modality-specific encoder for each modality, attempting to enable a LLM to comprehend images or videos through several projection layers. But their performances are inferior to dedicated video expert models such as Video-ChatGPT (Maaz et al., 2023). We attribute this phenomenon to the lack of *alignment before projection*. Because image features and video features reside in their own spaces, this poses a challenge for a LLM to learn their interactions from several poor projection layers. Some similar phenomenon such as *alignment before fusion* has been discussed by ALBEF (Li et al., 2021) and ViLT (Kim et al., 2021) in multi-model models. More recently, ImageBind-LLM (Han et al., 2023) focuses on enabling the LLM to simultaneously process multiple modal inputs by pre-aligning each modality to a common feature space (Girdhar et al., 2023). Based on a large image-language model, ImageBind-LLM converts other modalities into the most similar image features by retrieving from a training-free image cached database. However, the indirect alignment approach of ImageBind-LLM may lead to performance degradation, and the LLM has no knowledge of actual video data.

In this work, we introduce **Video-LLaVA**, a simple but powerful baseline for the LVLM simultaneously handling both images and videos. Specifically, As shown in Figure 1, Video-LLaVA initially aligns the representations of images and videos to a unified visual feature space. Since the visual representations are already aligned prior to projection, we employ a shared projection layer to map the unified visual representation for the LLM. To enhance computational efficiency, Video-LLaVA undergoes joint training of images and videos, achieving remarkable results with 1 training epoch.

As a result, The proposed Video-LLaVA greatly enhances the ability of the LLM to simultaneously understand both images and videos. For image understanding, Video-LLaVA surpasses advanced LVLMs such as mPLUG-owl-7B and InstructBLIP-7B in 5 image benchmarks. Additionally, utilizing 4 benchmark toolkits for a more comprehensive evaluation, Video-LLaVA-7B even outperforms IDEFICS-80B by 6.4% in MMBench. Moreover, similar trends can be observed in video understanding, where Video-LLaVA surpasses Video-ChatGPT by 5.8%, 9.9%, 18.6%, and 10.1% respectively on the MSVD, MSRVTT, TGIF, and ActivityNet video question-answering datasets. Extensive ablation experiments demonstrate that alignment before projection yields greater benefits. Additionally, joint training of images and videos can facilitate a unified visual representation in LLM comprehension.

We summarize our primary contributions as follows:

- We introduce **Video-LLaVA**, a powerful LVLM baseline. During the training process, Video-LLaVA binds visual signals to the language feature space, unifying visual representations, and proposes a solution to align before projection. We enable an LLM to perform visual reasoning capabilities on both images and videos simultaneously.
- Extensive experiments demonstrate that a unified visual representation benefits LLMs in learning to simultaneously handle both images and videos, validating the complementarity of modalities, showcasing significant superiority when compared to models specifically designed for either images or videos.

2 Related Work

2.1 Large Language Models

When the well-known commercial model ChatGPT (OpenAI, 2023) was introduced, the The AI community released open-source Large Language Models (LLMs) by instruction tuning and increasing model sizes. These include LLaMA (Touvron et al., 2023a), Vicuna (Chiang et al., 2023), Alpaca (Taori et al., 2023), and more recently, LLaMA 2 (Touvron et al., 2023b). These models are tuned with instruction sets to emulate conversations between humans and AI assistants. Furthermore, InstructGPT (Ouyang et al., 2022) is trained based on GPT-3 (Brown et al., 2020) with 175 billion parameters through aligning with human preferences. However, LLMs can only interact within text. In this work, we introduce Video-LLaVA, which builds upon the powerful reasoning capabilities of LLM to extend modality interactions to images and videos.

2.2 Large Vision-Language Models

When extending LLMs to multi-modal, especially involving images and videos, the main approaches can be categorized into two types in Table 1: *i)* treating LLM as a scheduler, *ii)* treating LLM as a decoder.

Methods	Image	Video	Pre-aligned	Joint
LLMs as scheduler				
VisualChatGPT	✔	✗	-	-
HuggingGPT	✔	✗	-	-
MM-REACT	✔	✔	-	-
ViperGPT	✔	✔	-	-
LLMs as decoder				
Mini-GPT4	✔	✗	-	✗
LLaVA	✔	✗	-	✗
Video-ChatGPT	✗	✔	-	✗
VideoChat	✔	✔	✗	✔
Video-LLaMA	✔	✔	✗	✔
ImageBind-LLM	✔	✔	✔	✗
Video-LLaVA (Ours)	✔	✔	✔	✔

Table 1: **Comparison between different Large Vision-Language Models.** For methods that treat LLMs as scheduler, they do not require pre-alignment and joint training.

LLMs as scheduler In the scheduler-based methods, various visual models are treated as plug-and-play modules. LLM schedules them according to the specific visual task requirements, like the assembly of building blocks. Some of these methods focus on images, such as VisualChatGPT (Wu et al., 2023) and HuggingGPT (Shen et al., 2023), while MM-REACT (Yang et al., 2023) and ViperGPT (Surís et al., 2023) can also handle videos. A key characteristic of these scheduler-based LVLMs is that they do not require end-to-end training, hence eliminating the need for pre-alignment and joint training of each modality.

LLMs as decoder Regarding the approach of treating LLM as a decoder, this is our primary focus. MiniGPT-4 (Zhu et al., 2023b) aligns image tokens to the input of the large language model through several linear projection layers. However, this alignment is weak and lacks feedback from human instructions. Subsequently, mPLUG-Owl (Ye et al., 2023) adopts a two-stage training approach. In the first stage, images are aligned with language using an auto-regressive pretraining style, and the second stage involves instruction tuning through using a human instruction dataset. With the increasing scale of large language model backends, approaches such as InstructBLIP (Dai et al., 2023) and LLaVA (Liu et al., 2023b,a) collecte the larger human instruction datasets to train a larger LVLMs (13B parameters). Each answer of instruction datasets strictly follow to the given instructions. Then they undergo end-to-end training using human instruction datasets, enabling the LLM with visual reasoning capabilities. Moreover, Video-ChatGPT (Maaz et al., 2023) design a 100k video instruction dataset, successfully empowering LLMs to comprehend videos. VideoChat (Li et al., 2023c) and Video-LLaMA (Zhang et al., 2023a) achieve this by conducting joint training, allowing LLMs to simultaneously handle images and videos. Expanding LLMs to additional visual modalities typically requires pre-alignment, as seen in LLaMA-Adapter (Zhang et al., 2023b; Gao et al., 2023) and ImageBind-LLM (Han et al., 2023). They bind other modalities to the image space through ImageBind's (Girdhar et al., 2023) modality encoder. These models have demonstrated that a unified feature space is advantageous for enhancing LLM's multi-modal reasoning capabilities. Distinguished from prior work, Video-LLaVA not only pre-aligns image and video features but also conducts joint training of images and videos, facilitating LLMs in learning multi-modal reasoning capabilities from a unified visual representation.

3 Video-LLaVA

3.1 Model Structure

Framework Overview As shown in Figure 2, Video-LLaVA consists of LanguageBind encoders $f_{\mathbf{V}}$ (Zhu et al., 2023a) to extract features from the raw visual signal (images or videos), a large language model $f_{\mathbf{L}}$ such as Vicuna, visual projection layers $f_{\mathbf{P}}$ and a word embedding layer $f_{\mathbf{T}}$. We initially obtain visual features using LanguageBind encoders. LanguageBind encoders are capable of mapping different modalities into the textual feature space, thereby providing us with a unified visual representation. Subsequently, the unified visual representation is encoded by shared projection layers, which is then combined with tokenized textual queries and fed into a large language model to generate corresponding responses.

United Visual Representation Our goal is to map images and videos into a shared feature space to enable the large language model to learn from a unified visual representation. We assume that the same information can be conveyed through multiple media. For example, a `running dog` can be expressed through language, a image or a video simultaneously. Therefore, we can compress information from different modalities into a common feature space, allowing the model to extract information

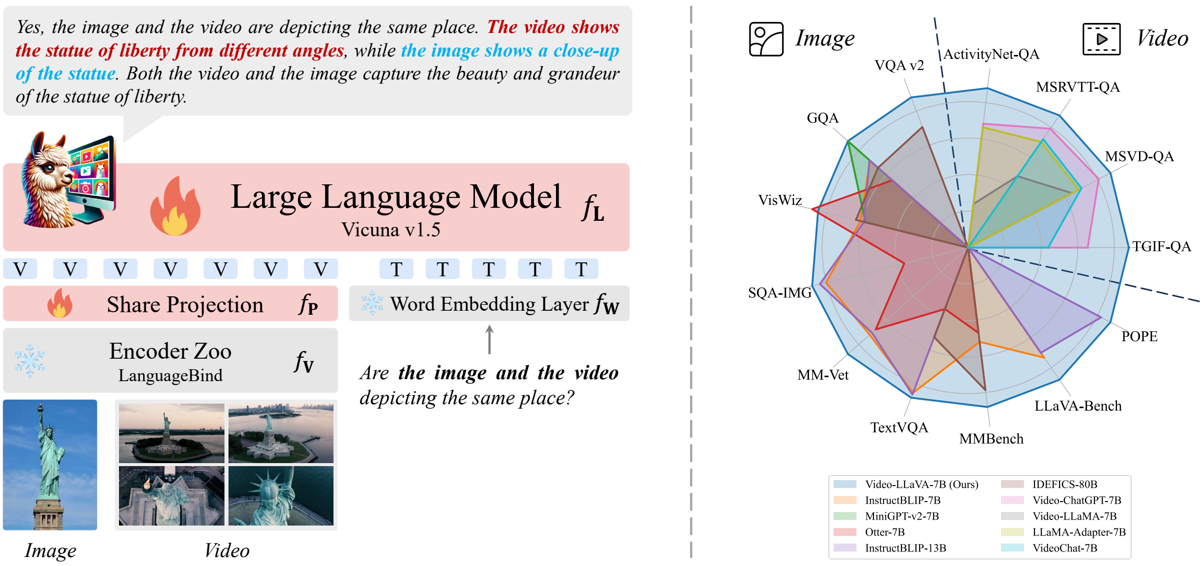

(a) Illustration of Video-LLaVA

(b) Performance comparison

Figure 2: **Training framework and performance.** Video-LLaVA exhibits remarkable interactive capabilities between images and videos, despite the absence of image-video pairs in the dataset. (a) The Video-LLaVA framework demonstrates a data flow that generates corresponding responses based on input instructions. (b) Video-LLaVA achieves superior performances on a broad range of 15 datasets across image and video.

from a dense feature space, facilitating modality interactions and complementarity. Hence, we chose the modality encoders from LanguageBind (Zhu et al., 2023a), which align images and videos with the textual feature space.

Alignment Before Projection Specifically, LanguageBind initializes from OpenCLIP (Ilharco et al., 2021), naturally aligning images and language in a shared feature space. Subsequently, it aligns video representations to the language space using 3 million video-text pairs from VIDAL-10M (Zhu et al., 2023a). By sharing a language feature space, the image and video representations ultimately converge into a unified visual feature space, which we refer to as emergent alignment of images and videos. Therefore, our video encoder and image encoder are initialized from the LanguageBind encoders zoo, pre-aligning the inputs for LLM and reducing the gap between representations of different visual signals. The unified visual representation is fed into LLM after passing through a shared projection layer.

3.2 Training Pipeline

Overall, the process of generating responses by Video-LLaVA is similar to that of a large language model (GPT series). Given a textual input $\mathbf{X}_{\mathrm{T}}$ and visual signals $\mathbf{X}_{\mathrm{V}}$, the input signals are encoded into a sequence of tokens according to Equation 1. By maximizing the likelihood probability in Equation 2, the model ultimately achieves multi-modal understanding capabilities.

$$\mathbf{Z}_{\mathrm{T}} = f_{\mathbf{T}}\left(\mathbf{X}_{\mathrm{T}}\right), \mathbf{Z}_{\mathrm{V}} = f_{\mathbf{P}}\left(f_{\mathbf{V}}\left(\mathbf{X}_{\mathrm{V}}\right)\right) \quad (1)$$

$$p\left(\mathbf{X}_{\mathrm{A}} \mid \mathbf{X}_{\mathrm{V}}, \mathbf{X}_{\mathrm{T}}\right) = \prod_{i=1}^{L} p_{\theta}\left(\mathbf{X}_{\mathrm{A}}^{[i]} \mid \mathbf{Z}_{\mathrm{V}}, \mathbf{Z}_{\mathrm{T}}^{[1:i-1]}\right) \quad (2)$$

where L is the length of the generated sequence $\mathbf{X}_{\mathrm{A}}$, and θ is a trainable parameter. We dynamically conduct joint training on images and videos, wherein a single batch contains both image and video samples simultaneously.

Understanding Training At this stage, the model is required to acquire the ability to interpret visual signals within a extensive image/video-text pair dataset. Each visual signal corresponds to a single round of conversation data $(\mathbf{X}_{\mathrm{q}}, \mathbf{X}_{\mathrm{a}})$, where $\mathbf{X}_{\mathrm{T}} = \mathbf{X}_{\mathrm{q}}$ and $\mathbf{X}_{\mathrm{a}}$ is the ground truth. The training objective of this stage is the original auto-regressive loss, where the model learns the basic ability to view the vision. We freeze the other parameters of the model during this process.

Instruction Tuning In this stage, the model is required to provide responses corresponding to different instructions. These instructions often involve more complex visual comprehension tasks, rather than just describing visual signals. Note that the conversation data $\left(\mathbf{X}_{\mathrm{q}}^{1}, \mathbf{X}_{\mathrm{a}}^{1}, \cdots, \mathbf{X}_{\mathrm{q}}^{N}, \mathbf{X}_{\mathrm{a}}^{N}\right)$ consists of multiple rounds.

$$\mathbf{X}_{\mathrm{T}}^{r} = \begin{cases} \mathbf{X}_{\mathrm{q}}^{1}, & r = 1 \\ \mathrm{Concat}(\mathbf{X}_{\mathrm{q}}^{r-1}, \mathbf{X}_{\mathrm{A}}^{r-1}, \mathbf{X}_{\mathrm{q}}^{r}), & r > 1 \end{cases} \tag{3}$$

where r represents the round number. As shown in Equation 3, when $r > 1$ we concatenate the conversations from all previous rounds with the current instruction as the input for this round. The training objective remains the same as in the previous stage. After this stage, the model learns to generate corresponding responses based on different instructions and requests. The LLM are also involved in training at this stage.

Zero-shot Image Question-answering To begin with, We evaluate our approach for image understanding on five academic image question-answering benchmarks. Compared to the state-of-the-art model InstructBLIP-7B, Video-LLaVA demonstrates powerful image understanding capabilities, outperforming across all five question-answering benchmarks. Additionally, Video-LLaVA exhibits competitive results compared to several more powerful LVLMs, which are tuned based on 13B or 65B LLM, such as surpassing InstructBLIP-13B by 14.7% on VisWiz, highlighting its strong understanding ability in natural visual environments.

4 Experiments

4.1 Experimental Setup

Model Settings We employ Vicuna-7B v1.5 as the large language model. The visual encoders are derived from LanguageBind, initialized from ViT-L/14. The text tokenizer is sourced from LLaMA, with approximately 32,000 classes. The share projection layers consist of 2 fully connected layers.

Data Details As shown in Figure 3, for the stage of understanding pretraining, we use a subset of 558K LAION-CC-SBU image-text pairs with BLIP (Li et al., 2022) captions, which is sourced from CC3M (Sharma et al., 2018) and filtered by Liu (Liu et al., 2023b). The video-text pairs are derived from a subset provided by Valley (Luo et al., 2023), and we have access to 702k out of a total of 703k pairs, originating from WebVid (Bain et al., 2021). For the stage of instruction tuning, We gathered instructional datasets from two sources, including a 665k image-text instruction dataset from LLaVA v1.5 (Liu et al., 2023a) and a 100k video-text instruction dataset from Video-ChatGPT.

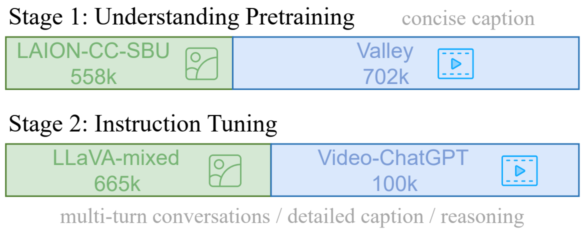

Figure 3: **Data composition for training Video-LLaVA.** The dataset for stage 1 consists of single-turn conversation, focusing on concise visual descriptions. In stage 2, the dataset comprises multi-turn conversations, emphasizing complex visual reasoning abilities.

Training Details In the training process, we resize and crop each image, resulting in a size of 224×224 for each processed image. We uniformly sample 8 frames from each video, and each frame undergoes image pre-processing. The data in each batch is a random combination of images and videos. In the first stage, we train for one epoch with a batch size of 256, using the AdamW optimizer with a cosine learning rate schedule. In the second stage, we reduce the batch size to 128. The initial learning rate for both stages is set to 1e-3, with a warmup ratio of 0.03. Additional hyper-parameter settings can be found in the appendix.

4.2 Quantitative Evaluation

Zero-shot Video Understanding As shown in Table 2, we conduct a quantitative assessment of the video question-answering capabilities of large video-language models on four datasets, including MSVD-QA (Chen and Dolan, 2011), MSRVTT-QA (Xu et al., 2016), TGIF-QA (Jang et al., 2017) and ActivityNet-QA (Yu et al., 2019). The evaluation pipeline for video understanding follows Video-ChatGPT. We report the accuracy and score, which is assessed using GPT-Assistant. Video-LLaVA consistently outperforms Video-ChatGPT in terms of question-answering accuracy, which is an advanced large video-language model. Moreover, Video-LLaVA surpasses the powerful baseline of Video-ChatGPT by 5.8%, 9.9%, 18.6%, and 10.1% on MSRVTT, MSVD, TGIF, and ActivityNet, respectively. Additionally, we conduct comparisons with the recent SOTA model, Chat-UniVi (Jin et al., 2023). Despite Chat-UniVi utilizing more datasets such as MIMIC-IT (Li et al., 2023a), Video-LLaVA still demonstrate compet-

Methods	LLM size	MSVD-QA		MSRVTT-QA		TGIF-QA		ActivityNet-QA	
		Accuracy	Score	Accuracy	Score	Accuracy	Score	Accuracy	Score
FrozenBiLM	1B	32.2	-	16.8	-	41.0	-	24.7	-
VideoChat	7B	56.3	2.8	45.0	2.5	34.4	2.3	-	2.2
LLaMA-Adapter	7B	54.9	3.1	43.8	2.7	-	-	34.2	2.7
Video-LLaMA	7B	51.6	2.5	29.6	1.8	-	-	12.4	1.1
Video-ChatGPT	7B	64.9	3.3	49.3	2.8	51.4	3.0	35.2	2.7
Chat-UniVi	7B	65.0	3.6	54.6	3.1	60.3	3.4	**45.8**	3.2
Video-LLaVA	7B	**70.7**	**3.9**	**59.2**	**3.5**	**70.0**	**4.0**	45.3	**3.3**

Table 2: **Comparison between different LVLMs on video reasoning benchmarks**. We employ ChatGPT-Assistant to evaluate the performance following Video-ChatGPT (Maaz et al., 2023). The version of ChatGPT is “gpt-3.5-turbo”.

Methods	LLM	Res.	Image Question Answering					Benchmark Toolkit			
			VQA^{v2}	GQA	VisWiz	SQA^{I}	VQA^{T}	POPE	MMB	LLaVA^{W}	MM-Vet
LLaVA-1.5	Vicuna-7B	336	-	62.0*	-	-	-	-	-	-	30.5
BLIP-2	Vicuna-13B	224	41.0	41.0	19.6	61.0	42.5	85.3	-	38.1	22.4
InstructBLIP	Vicuna-13B	224	-	49.5	33.4	63.1	50.7	78.9	-	58.2	25.6
IDEFICS-80B	LLaMA-65B	224	60.0	45.2	36.0	-	30.9	-	54.5	-	-
MiniGPT-4	LLaMA-7B	224	-	30.8	47.5	25.4	19.4	-	23.0	-	22.1
IDEFICS-9B	LLaMA-7B	224	50.9	38.4	35.5	-	25.9	-	48.2	-	-
mPLUG-Owl	LLaMA-7B	224	-	14.0	39.0	2.8	38.8	-	46.6	-	-
Otter	LLaMA-7B	224	-	38.1	**50.0**	27.2	21.2	-	32.6	-	24.6
InstructBLIP	Vicuna-7B	224	-	49.2	34.5	60.5	50.1	-	36.0	60.9	26.2
Video-LLaVA	Vicuna-7B	224	**74.7***	**60.3***	48.1	**66.4**	**51.8**	**84.4**	**60.9**	**73.1**	**32.0**

Table 3: **Comparison between different LVLMs on image understanding benchmarks.** Res. indicate input image resolution. Benchmark names are abbreviated due to page limitations. VQA-v2 (Goyal et al., 2017); GQA (Hudson and Manning, 2019); VisWiz (Gurari et al., 2018); SQA^{I}: ScienceQA-IMG (Lu et al., 2022); VQA^{T}: TextVQA (Singh et al., 2019); POPE (Li et al., 2023d); MMB: MMBench (Liu et al., 2023c); LLaVA^{W}: LLaVA-Bench (In-the-Wild) (Liu et al., 2023b); MM-Vet (Yu et al., 2023). * donates that there is some overlap in the training data.

itive results, surpassing Chat-UniVi on MSVD, MSRVTT, and TGIF datasets. In summary, these results validate Video-LLaVA's ability to comprehend videos and provide contextually appropriate responses based on instructions.

Zero-shot Image Question-answering As shown in Table 3, we evaluate our approach for image understanding on five academic image question-answering benchmarks. Compared to the state-of-the-art model InstructBLIP-7B, Video-LLaVA demonstrates powerful image understanding capabilities, outperforming across all five question-answering benchmarks. Additionally, Video-LLaVA exhibits competitive results compared to several more powerful LVLMs, which are tuned based on 13B or 65B LLM, such as surpassing InstructBLIP-13B by 14.7% on VisWiz, highlighting its strong understanding ability in natural visual environments. Furthermore, to ensure a fair comparison, we replace the image encoder in LLaVA-1.5 with the LanguageBind-Image encoder, called LLaVA-1.5†. This demonstrates that the performance improvement observed in Video-LLaVA is not solely attributed to a stronger image encoder.

Evaluation under Benchmark Toolkits Additionally, we evaluate LVLMs using several benchmark toolkits for visual instruction tuning. These benchmark toolkits provide a detailed assessment of the model's capabilities through robust evaluation metrics. Video-LLaVA outperform InstructBLIP-7B by 24.9%, 12.2%, and 5.8% on MMBench, LLaVA-Bench, and MM-Vet, respectively. It is worth noting that Video-LLaVA-7B still demonstrates advanced performance compared to larger LLM models, surpassing InstructBLIP-13B by 6.4% on MM-Vet and IDEFICS-80B (Laurençon et al., 2023) by 6.4% on MMBench. These results demonstrate that Video-LLaVA exhibits a strong understanding of semantic aspects of scenes, enabling it to answer open-ended and free-form natural language questions about images.

Object Hallucination Evaluation As shown in Table 4, we report evaluation results for zero-shot object hallucinations, utilizing a evaluation pipeline

Methods	LLM	Adersarial			Popular			Random		
		Accuracy	F1-Score	Yes	Accuracy	F1-Score	Yes	Accuracy	F1-Score	Yes
MiniGPT-4	Vicuna-13B	66.6	71.4	66.7	68.3	72.2	64.1	77.8	78.9	54.8
InstructBLIP	Vicuna-13B	74.4	78.5	69.0	81.4	83.5	62.6	**88.7**	**89.3**	55.2
MM-GPT	LLaMA-7B	50.0	66.7	100.0	50.0	66.7	100.0	50.0	66.7	100.0
Video-LLaVA	Vicuna-7B	**81.6**	**80.8**	45.8	**85.3**	**84.0**	42.1	86.2	85.2	42.0

Table 4: **Zero-shot object hallucination evaluation results** are reported for three POPE evaluation settings. "Yes" indicates the proportion of positive responses to the given question.

derived from a polling-based query method (Li et al., 2023d). Video-LLaVA demonstrates competitive performance across three subsets: random, popular, and adversarial. Specifically, when compared to the 7B foundation model, Video-LLaVA consistently outperforms MM-GPT (Gong et al., 2023) across all three POPE hallucination evaluation subsets. Furthermore, when benchmarked against the larger 13B LLM, Video-LLaVA even surpasses Mini-GPT4 comprehensively. The successful performance of Video-LLaVA in object hallucination detection validates the consistency between unified visual representations and the generation of textual descriptions.

4.3 Ablation Results

4.3.1 Alignment Before Projection

To validate the performance degradation caused by separated visual representation, we conduct experiments to to explore the performance of the LLM learning from different visual representations. We define the use of LanguageBind image encoder as unified visual representation while the MAE encoder (He et al., 2022) is separated visual representation, which is a well-known and effective image feature extractor. We only replace the image encoder with the MAE image encoder of the same scale and keep the LanguageBind video encoder. We compare the united visual representation and the separated visual representation on 13 benchmarks, including 9 image understanding benchmarks and 4 video understanding benchmarks.

For Image Understanding The unified visual representation demonstrates strong performance, surpassing the separated visual representation comprehensively across 5 image question-answering datasets and 4 benchmark toolkits in Figure 4. Additionally, we observe a significant margin of performance improvement in the unified visual representation on the POPE, MMBench, LLaVA-Bench, and MM-Vet benchmark toolkits. This highlights that the unified visual representation not only enhances performance in image question-answering but also provides benefits in other aspects of image understanding, such as reducing object hallucination and improving OCR capabilities.

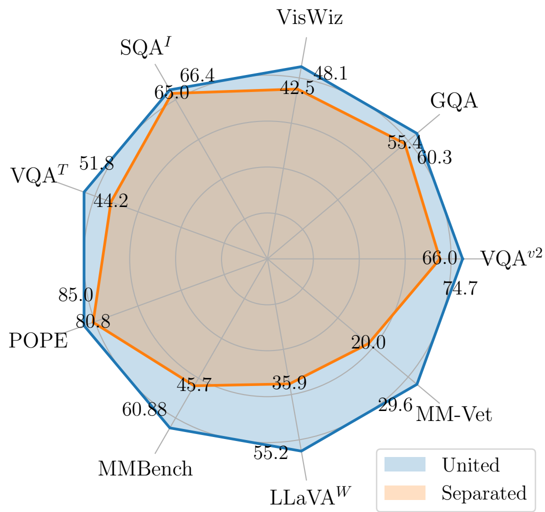

Figure 4: **Effect of alignment before projection on image.** "United" refers to the unified visual representation, while "Separated" refers to the separated visual representation.

For Video Understanding Due to replacing the image encoder with the MAE encoder, the video features and image features are no longer unified during LLM's initial learning of visual representations. In Figure 5, compared to separated visual representation, the united visual representation significantly improves performance across 4 video question-answering datasets. Separated visual representations not only exhibit lower accuracy in question-answering, but also demonstrate a similar trend in answer scores. These results demonstrate that the unified visual representation can help the LLM further learn and understand videos.

4.3.2 Joint Training

This subsection aims to validate the complementarity of images and videos during joint training, which can mutually enhance the LLM's understand-

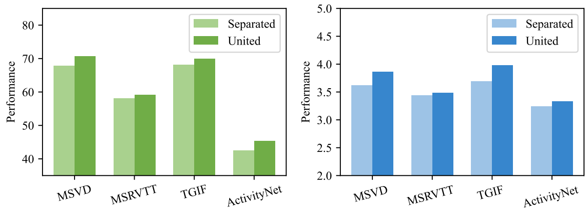

(a) Accuracy of question-answering (b) Score of question-answering

Figure 5: **Effect of alignment before projection on video.** We validate and report the accuracy and score on four video question-answering datasets.

ing of images and videos based on a unified visual representation.

For Image Understanding As shown in Figure 6, We find that both images and videos benefit from joint training, demonstrating mutual improvement in visual understanding. In comparison to LLaVA, we conduct evaluations of image question-answering on VisWiz, focusing on three aspects: *i)* unanswerable, predicting whether visual questions are unanswerable; *ii)* number, tasks related to numerical understanding; and *iii)* other, additional visual understanding tasks. Video-LLaVA outperform LLaVA in unanswerable and number tasks, indicating that joint training with videos alleviates the object hallucination in images and enhances the understanding of numerical signals in images. A similar trend is observed on the LLaVA-Bench, where video data significantly improves LLM's performance in complex reasoning and image conversation tasks.

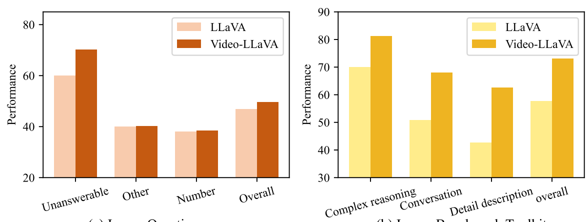

(a) Image Question-answer (b) Image Benchmark Toolkit

Figure 6: **Effect of joint training on image.** (a) We evaluate on the image question answering dataset, namely VisWiz. (b) We evaluate on a benchmark toolkit proposed by LLaVA, namely LLaVA-Bench (In-the-Wild). We reproduce the results of LLaVA at a resolution of 224×224 for a fair comparison.

For Video Understanding In Table 5, we evaluate our model on four video question-answering datasets. Compared to Video-LLaVA* without image in training, the model trained with joint images and videos achieves comprehensive improvements across all four video datasets. These results demonstrate that joint training of images and videos facilitates LLM's understanding of visual representations.

Methods	**MSVD**	**MSRVTT**	**TGIF**	**ActivityNet**
Video-LLaVA*	64.8	58.3	67.8	40.7
Joint with Image	70.7	59.2	70.0	45.3
Δ *Acc.*	*+ 5.9%*	*+ 0.9%*	*+ 2.2%*	*+ 4.6%*

Table 5: **Effect of joint training on video.** We evaluate on four video question-answering datasets. * denotes that we utilized only video data in both the first and second stages.

5 Conclusion and Future Directions

In this work, we introduce Video-LLaVA, a simple but powerful large visual-language baseline model. We propose a novel framework to address the issue of misalignment before projection, utilizing a LanguageBind encoder to pre-bind visual signals into the language feature space. To enable a LLM to comprehend both images and videos simultaneously, we conduct joint training on images and videos, allowing the LLM to learn multi-modal interactions from a unified visual representation. Extensive experiments demonstrate that joint training on images and videos mutually benefits performance. Furthermore, we validate that aligning visual representations before projection aids LLM learning. Remarkably, LLM, after learning from a unified visual representation, exhibits the remarkable ability to simultaneously engage with both images and videos, showcasing a powerful comprehension of unified visual concepts. These results collectively demonstrate the effectiveness of the Video-LLaVA training framework. As a unified visual training framework, the performance of Video-LLaVA even surpasses that of expert models designed specifically for images or videos.

Future work While Video-LLaVA exhibits strong competitiveness in both images and videos, we observe that it faces difficulty in grasping temporal relationships and spatio-temporal localization. Video-LLaVA can serve as a baseline to extend to additional visual-related modalities, such as depth and infrared images. Additionally, we could explore how to incorporate timestamp embeddings effectively, enabling large visual-language models to answer questions related to temporal relationships.

References

Jean-Baptiste Alayrac, Jeff Donahue, Pauline Luc, Antoine Miech, Iain Barr, Yana Hasson, Karel Lenc, Arthur Mensch, Katherine Millican, Malcolm Reynolds, et al. 2022. Flamingo: a visual language model for few-shot learning. *Advances in Neural Information Processing Systems*, 35:23716–23736.

Rohan Anil, Andrew M Dai, Orhan Firat, Melvin Johnson, Dmitry Lepikhin, Alexandre Passos, Siamak Shakeri, Emanuel Taropa, Paige Bailey, Zhifeng Chen, et al. 2023. Palm 2 technical report. *arXiv preprint arXiv:2305.10403*.

Max Bain, Arsha Nagrani, Gül Varol, and Andrew Zisserman. 2021. Frozen in time: A joint video and image encoder for end-to-end retrieval. In *Proceedings of the IEEE/CVF International Conference on Computer Vision*, pages 1728–1738.

Bin Bi, Chenliang Li, Chen Wu, Ming Yan, Wei Wang, Songfang Huang, Fei Huang, and Luo Si. 2020. Palm: Pre-training an autoencoding&autoregressive language model for context-conditioned generation. *arXiv preprint arXiv:2004.07159*.

Tom Brown, Benjamin Mann, Nick Ryder, Melanie Subbiah, Jared D Kaplan, Prafulla Dhariwal, Arvind Neelakantan, Pranav Shyam, Girish Sastry, Amanda Askell, et al. 2020. Language models are few-shot learners. *Advances in neural information processing systems*, 33:1877–1901.

David Chen and William B Dolan. 2011. Collecting highly parallel data for paraphrase evaluation. In *Proceedings of the 49th annual meeting of the association for computational linguistics: human language technologies*, pages 190–200.

Feilong Chen, Minglun Han, Haozhi Zhao, Qingyang Zhang, Jing Shi, Shuang Xu, and Bo Xu. 2023. X-llm: Bootstrapping advanced large language models by treating multi-modalities as foreign languages. *arXiv preprint arXiv:2305.04160*.

Wei-Lin Chiang, Zhuohan Li, Zi Lin, Ying Sheng, Zhanghao Wu, Hao Zhang, Lianmin Zheng, Siyuan Zhuang, Yonghao Zhuang, Joseph E Gonzalez, et al. 2023. Vicuna: An open-source chatbot impressing gpt-4 with 90%* chatgpt quality. *See https://vicuna. lmsys. org (accessed 14 April 2023)*.

Wenliang Dai, Junnan Li, Dongxu Li, Anthony Meng Huat Tiong, Junqi Zhao, Weisheng Wang, Boyang Li, Pascale Fung, and Steven Hoi. 2023. Instructblip: Towards general-purpose vision-language models with instruction tuning. *Preprint*, arXiv:2305.06500.

Peng Gao, Jiaming Han, Renrui Zhang, Ziyi Lin, Shijie Geng, Aojun Zhou, Wei Zhang, Pan Lu, Conghui He, Xiangyu Yue, et al. 2023. Llama-adapter v2: Parameter-efficient visual instruction model. *arXiv preprint arXiv:2304.15010*.

Rohit Girdhar, Alaaeldin El-Nouby, Zhuang Liu, Mannat Singh, Kalyan Vasudev Alwala, Armand Joulin, and Ishan Misra. 2023. Imagebind: One embedding space to bind them all. In *Proceedings of the IEEE/CVF Conference on Computer Vision and Pattern Recognition*, pages 15180–15190.

Tao Gong, Chengqi Lyu, Shilong Zhang, Yudong Wang, Miao Zheng, Qian Zhao, Kuikun Liu, Wenwei Zhang, Ping Luo, and Kai Chen. 2023. Multimodal-gpt: A vision and language model for dialogue with humans. *arXiv preprint arXiv:2305.04790*.

Yash Goyal, Tejas Khot, Douglas Summers-Stay, Dhruv Batra, and Devi Parikh. 2017. Making the v in vqa matter: Elevating the role of image understanding in visual question answering. In *Proceedings of the IEEE conference on computer vision and pattern recognition*, pages 6904–6913.

Danna Gurari, Qing Li, Abigale J Stangl, Anhong Guo, Chi Lin, Kristen Grauman, Jiebo Luo, and Jeffrey P Bigham. 2018. Vizwiz grand challenge: Answering visual questions from blind people. In *Proceedings of the IEEE conference on computer vision and pattern recognition*, pages 3608–3617.

Jiaming Han, Renrui Zhang, Wenqi Shao, Peng Gao, Peng Xu, Han Xiao, Kaipeng Zhang, Chris Liu, Song Wen, Ziyu Guo, et al. 2023. Imagebind-llm: Multi-modality instruction tuning. *arXiv preprint arXiv:2309.03905*.

Kaiming He, Xinlei Chen, Saining Xie, Yanghao Li, Piotr Dollár, and Ross Girshick. 2022. Masked autoencoders are scalable vision learners. In *Proceedings of the IEEE/CVF conference on computer vision and pattern recognition*, pages 16000–16009.

Drew A Hudson and Christopher D Manning. 2019. Gqa: A new dataset for real-world visual reasoning and compositional question answering. In *Proceedings of the IEEE/CVF conference on computer vision and pattern recognition*, pages 6700–6709.

Gabriel Ilharco, Mitchell Wortsman, Ross Wightman, Cade Gordon, Nicholas Carlini, Rohan Taori, Achal Dave, Vaishaal Shankar, Hongseok Namkoong, John Miller, Hannaneh Hajishirzi, Ali Farhadi, and Ludwig Schmidt. 2021. Openclip. If you use this software, please cite it as below.

Yunseok Jang, Yale Song, Youngjae Yu, Youngjin Kim, and Gunhee Kim. 2017. Tgif-qa: Toward spatio-temporal reasoning in visual question answering. In *Proceedings of the IEEE conference on computer vision and pattern recognition*, pages 2758–2766.

Peng Jin, Ryuichi Takanobu, Caiwan Zhang, Xiaochun Cao, and Li Yuan. 2023. Chat-univi: Unified visual representation empowers large language models with image and video understanding. *arXiv preprint arXiv:2311.08046*.

Wonjae Kim, Bokyung Son, and Ildoo Kim. 2021. Vilt: Vision-and-language transformer without convolution or region supervision. In *International Conference on Machine Learning*, pages 5583–5594. PMLR.

Hugo Laurençon, Lucile Saulnier, Léo Tronchon, Stas Bekman, Amanpreet Singh, Anton Lozhkov, Thomas Wang, Siddharth Karamcheti, Alexander M. Rush, Douwe Kiela, Matthieu Cord, and Victor Sanh. 2023. Obelics: An open web-scale filtered dataset of interleaved image-text documents. *Preprint*, arXiv:2306.16527.

Bo Li, Yuanhan Zhang, Liangyu Chen, Jinghao Wang, Jingkang Yang, and Ziwei Liu. 2023a. Otter: A multi-modal model with in-context instruction tuning. *arXiv preprint arXiv:2305.03726*.

Junnan Li, Dongxu Li, Silvio Savarese, and Steven Hoi. 2023b. Blip-2: Bootstrapping language-image pre-training with frozen image encoders and large language models. *arXiv preprint arXiv:2301.12597*.

Junnan Li, Dongxu Li, Caiming Xiong, and Steven Hoi. 2022. Blip: Bootstrapping language-image pre-training for unified vision-language understanding and generation. In *International Conference on Machine Learning*, pages 12888–12900. PMLR.

Junnan Li, Ramprasaath Selvaraju, Akhilesh Gotmare, Shafiq Joty, Caiming Xiong, and Steven Chu Hong Hoi. 2021. Align before fuse: Vision and language representation learning with momentum distillation. *Advances in neural information processing systems*, 34:9694–9705.

KunChang Li, Yinan He, Yi Wang, Yizhuo Li, Wenhai Wang, Ping Luo, Yali Wang, Limin Wang, and Yu Qiao. 2023c. Videochat: Chat-centric video understanding. *arXiv preprint arXiv:2305.06355*.

Yifan Li, Yifan Du, Kun Zhou, Jinpeng Wang, Wayne Xin Zhao, and Ji-Rong Wen. 2023d. Evaluating object hallucination in large vision-language models. *arXiv preprint arXiv:2305.10355*.

Haotian Liu, Chunyuan Li, Yuheng Li, and Yong Jae Lee. 2023a. Improved baselines with visual instruction tuning. *arXiv preprint arXiv:2310.03744*.

Haotian Liu, Chunyuan Li, Qingyang Wu, and Yong Jae Lee. 2023b. Visual instruction tuning. *arXiv preprint arXiv:2304.08485*.

Yuan Liu, Haodong Duan, Yuanhan Zhang, Bo Li, Songyang Zhang, Wangbo Zhao, Yike Yuan, Jiaqi Wang, Conghui He, Ziwei Liu, et al. 2023c. Mmbench: Is your multi-modal model an all-around player? *arXiv preprint arXiv:2307.06281*.

Pan Lu, Swaroop Mishra, Tanglin Xia, Liang Qiu, Kai-Wei Chang, Song-Chun Zhu, Oyvind Tafjord, Peter Clark, and Ashwin Kalyan. 2022. Learn to explain: Multimodal reasoning via thought chains for science question answering. *Advances in Neural Information Processing Systems*, 35:2507–2521.

Ruipu Luo, Ziwang Zhao, Min Yang, Junwei Dong, Minghui Qiu, Pengcheng Lu, Tao Wang, and Zhongyu Wei. 2023. Valley: Video assistant with large language model enhanced ability. *arXiv preprint arXiv:2306.07207*.

Chenyang Lyu, Minghao Wu, Longyue Wang, Xinting Huang, Bingshuai Liu, Zefeng Du, Shuming Shi, and Zhaopeng Tu. 2023. Macaw-llm: Multi-modal language modeling with image, audio, video, and text integration. *arXiv preprint arXiv:2306.09093*.

Muhammad Maaz, Hanoona Rasheed, Salman Khan, and Fahad Shahbaz Khan. 2023. Video-chatgpt: Towards detailed video understanding via large vision and language models. *arXiv preprint arXiv:2306.05424*.

OpenAI. 2023. Gpt-4 technical report. *Preprint*, arXiv:2303.08774.

Long Ouyang, Jeffrey Wu, Xu Jiang, Diogo Almeida, Carroll Wainwright, Pamela Mishkin, Chong Zhang, Sandhini Agarwal, Katarina Slama, Alex Ray, et al. 2022. Training language models to follow instructions with human feedback. *Advances in Neural Information Processing Systems*, 35:27730–27744.

Teven Le Scao, Angela Fan, Christopher Akiki, Ellie Pavlick, Suzana Ilić, Daniel Hesslow, Roman Castagné, Alexandra Sasha Luccioni, François Yvon, Matthias Gallé, et al. 2022. Bloom: A 176b-parameter open-access multilingual language model. *arXiv preprint arXiv:2211.05100*.

Piyush Sharma, Nan Ding, Sebastian Goodman, and Radu Soricut. 2018. Conceptual captions: A cleaned, hypernymed, image alt-text dataset for automatic image captioning. In *Proceedings of the 56th Annual Meeting of the Association for Computational Linguistics (Volume 1: Long Papers)*, pages 2556–2565.

Yongliang Shen, Kaitao Song, Xu Tan, Dongsheng Li, Weiming Lu, and Yueting Zhuang. 2023. Hugginggpt: Solving ai tasks with chatgpt and its friends in huggingface. *arXiv preprint arXiv:2303.17580*.

Amanpreet Singh, Vivek Natarajan, Meet Shah, Yu Jiang, Xinlei Chen, Dhruv Batra, Devi Parikh, and Marcus Rohrbach. 2019. Towards vqa models that can read. In *Proceedings of the IEEE/CVF conference on computer vision and pattern recognition*, pages 8317–8326.

Dídac Surís, Sachit Menon, and Carl Vondrick. 2023. Vipergpt: Visual inference via python execution for reasoning. *arXiv preprint arXiv:2303.08128*.

Rohan Taori, Ishaan Gulrajani, Tianyi Zhang, Yann Dubois, Xuechen Li, Carlos Guestrin, Percy Liang, and Tatsunori B Hashimoto. 2023. Stanford alpaca: An instruction-following llama model.

Hugo Touvron, Thibaut Lavril, Gautier Izacard, Xavier Martinet, Marie-Anne Lachaux, Timothée Lacroix, Baptiste Rozière, Naman Goyal, Eric Hambro, Faisal

Azhar, et al. 2023a. Llama: Open and efficient foundation language models. *arXiv preprint arXiv:2302.13971*.

Hugo Touvron, Louis Martin, Kevin Stone, Peter Albert, Amjad Almahairi, Yasmine Babaei, Nikolay Bashlykov, Soumya Batra, Prajjwal Bhargava, Shruti Bhosale, et al. 2023b. Llama 2: Open foundation and fine-tuned chat models. *arXiv preprint arXiv:2307.09288*.

Chenfei Wu, Shengming Yin, Weizhen Qi, Xiaodong Wang, Zecheng Tang, and Nan Duan. 2023. Visual chatgpt: Talking, drawing and editing with visual foundation models. *arXiv preprint arXiv:2303.04671*.

Jun Xu, Tao Mei, Ting Yao, and Yong Rui. 2016. Msr-vtt: A large video description dataset for bridging video and language. In *Proceedings of the IEEE conference on computer vision and pattern recognition*, pages 5288–5296.

Zhengyuan Yang, Linjie Li, Jianfeng Wang, Kevin Lin, Ehsan Azarnasab, Faisal Ahmed, Zicheng Liu, Ce Liu, Michael Zeng, and Lijuan Wang. 2023. Mm-react: Prompting chatgpt for multimodal reasoning and action. *arXiv preprint arXiv:2303.11381*.

Qinghao Ye, Haiyang Xu, Guohai Xu, Jiabo Ye, Ming Yan, Yiyang Zhou, Junyang Wang, Anwen Hu, Pengcheng Shi, Yaya Shi, et al. 2023. mplug-owl: Modularization empowers large language models with multimodality. *arXiv preprint arXiv:2304.14178*.

Weihao Yu, Zhengyuan Yang, Linjie Li, Jianfeng Wang, Kevin Lin, Zicheng Liu, Xinchao Wang, and Lijuan Wang. 2023. Mm-vet: Evaluating large multimodal models for integrated capabilities. *arXiv preprint arXiv:2308.02490*.

Zhou Yu, Dejing Xu, Jun Yu, Ting Yu, Zhou Zhao, Yueting Zhuang, and Dacheng Tao. 2019. Activitynet-qa: A dataset for understanding complex web videos via question answering. In *Proceedings of the AAAI Conference on Artificial Intelligence*, volume 33, pages 9127–9134.

Hang Zhang, Xin Li, and Lidong Bing. 2023a. Video-llama: An instruction-tuned audio-visual language model for video understanding. *arXiv preprint arXiv:2306.02858*.

Renrui Zhang, Jiaming Han, Aojun Zhou, Xiangfei Hu, Shilin Yan, Pan Lu, Hongsheng Li, Peng Gao, and Yu Qiao. 2023b. Llama-adapter: Efficient fine-tuning of language models with zero-init attention. *arXiv preprint arXiv:2303.16199*.

Bin Zhu, Bin Lin, Munan Ning, Yang Yan, Jiaxi Cui, HongFa Wang, Yatian Pang, Wenhao Jiang, Junwu Zhang, Zongwei Li, et al. 2023a. Languagebind: Extending video-language pretraining to n-modality by language-based semantic alignment. *arXiv preprint arXiv:2310.01852*.

Deyao Zhu, Jun Chen, Xiaoqian Shen, Xiang Li, and Mohamed Elhoseiny. 2023b. Minigpt-4: Enhancing vision-language understanding with advanced large language models. *arXiv preprint arXiv:2304.10592*.

A Appendix

A.1 Training Setting

We show some training settings as shown in Table 6. video encoder and image encoder are not trained in both stages. The projection layer consists of 2 linear layers with a GeLU activation function between them. Image and video share the projection layer.

Table 6: Training setting.

Config	Pretraining	Instruction tuning
Video encoder	LanguageBind-Video-LoRA-800M	
Image encoder	LanguageBind-Image-600M	
LLM	Vicuna v1.5-7B (Chiang et al., 2023)	
Optimizer	AdamW	
Deepspeed	Zero2	
Epochs	1	
Vision select layer	-2	
Weight decay	0.0	
Warmup ratio	0.03	
Learning rate schedule	cosine decay	
Learning rate	1e-3	2e-5
Batch size	256	128

A.2 Limitation

While Video-LLaVA exhibits strong competitiveness in both images and videos, we still observed some limitations of Video-LLaVA. To begin with, Video-LLaVA performs moderately in understanding long videos. In Table 2, Chat-UniVi surpasses 0.5 on ActivityNet-QA because Video-LLaVA only utilizes uniformly sampled 8 frames to comprehend the video, which results in the loss of detailed information from long videos. Additionally, training Video-LLaVA is computationally expensive, requiring 3-4 days to complete the training process on 8 A100-80G GPUs.

A.3 Broader Impacts

While Video-LLaVA holds great potential and application value in multi-modal understanding, it may also have some negative social impacts:

- Information credibility: Video-LLaVA can generate realistic texts, including false information and misleading content.
- Bias and discrimination: The training data for Video-LLaVA often comes from the internet, where various biases and discriminatory content may exist. If these unequal patterns are learned and amplified by the model, they may be reflected in the generated responses.
- Social influence: People may become overly reliant on Video-LLaVA for information and problem-solving, instead of actively thinking and seeking multiple sources of information. This can lead to increased dependency, reduced autonomy in thinking, and judgment skills.

A.4 Licenses

The majority of this project is released under the Apache 2.0 license. The service is a research preview intended for non-commercial use only, subject to the model License of LLaMA (Touvron et al., 2023a).

A.5 Exhibition Board

We show some **unselected** samples here, and these videos are sourced from Video-ChatGPT.

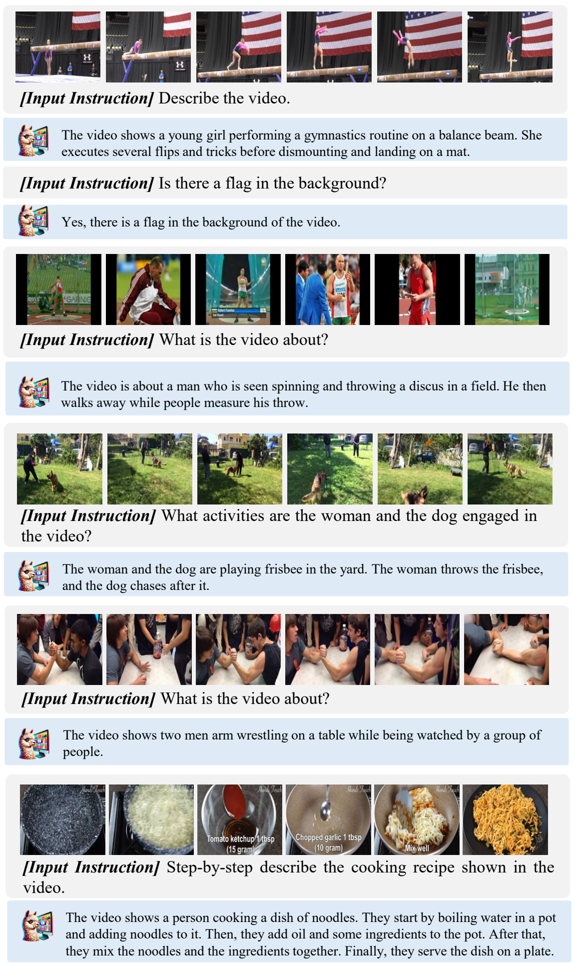

Figure 7: Samples of Video-LLaVA in video understanding.

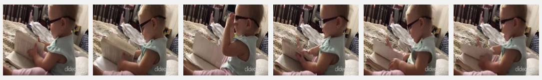

[Input Instruction] Why is this video funny?

The video is funny because the baby is playing with a Wii remote, which is not a toy typically associated with babies. The baby's actions are also humorous, such as pointing to the camera and making faces, which adds to the overall amusement of the video.

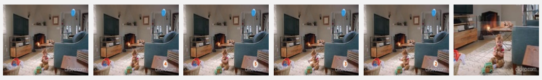

[Input Instruction] Can you identify any safety hazards in this video?

Yes, the baby is playing with a toy truck and a toy car, which could pose a safety risk if they are not supervised. However, the baby is sitting on the floor, so there is less risk of injury compared to if they were playing with the toys on a higher surface.

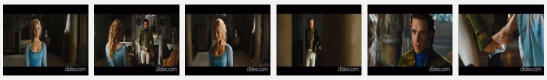

[Input Instruction] Create a short fairy tale with a moral lesson inspired by the video.

Once upon a time, in a kingdom far away, there lived a beautiful princess named Rose. She was known for her kindness and beauty, and everyone loved her. One day, a handsome prince named Leo came to visit the kingdom. He was fascinated by Rose's beauty and decided to stay in the kingdom. However, Rose's jealous sister, Lily, did not like the attention Leo was giving her sister. She tried to harm Rose, but Leo saved her and they fell in love. The kingdom celebrated their love and they lived happily ever after. The moral of the story is that true love conquers all and that jealousy can lead to harmful consequences.

[Input Instruction] Describe the video.

The video shows a person preparing a dish with peppers and oranges. They slice the peppers and oranges and lay them out on a table. The person then proceeds to cut the peppers and oranges into strips and lays them out on a piece of wax paper. They use a knife to cut the peppers and oranges into strips and lay them out on a piece of wax paper. The person then uses a spoon to mix the peppers and oranges together. The video ends with the person cutting the peppers and oranges into strips and laying them out on a piece of wax paper.

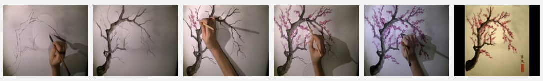

[Input Instruction] What is the main focus of the video.

The main focus of the video is the process of creating a painting of a tree using various techniques and colors. The video shows the artist's hand holding a paintbrush and using it to create the tree, as well as the use of different colors and techniques to create the painting.

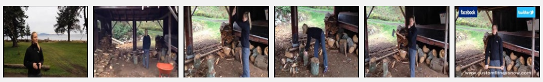

[Input Instruction] What does the woman use to split the logs and how does she do it?

The woman uses an ax to split the logs. She holds the ax in her hand and swings it down onto the log. She repeats this process several times, splitting the log into smaller pieces.

Figure 8: Samples of Video-LLaVA in video understanding.

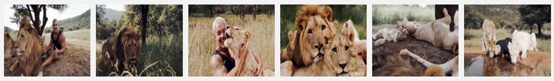

[Input Instruction] What is strange about this video?

The video is strange because it shows a man sitting next to a lion and a lion laying down next to a man. The man is also seen petting a lion in the grass.

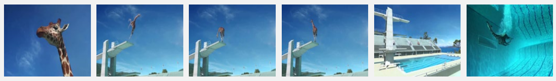

[Input Instruction] What is unusual about this video?

The unusual aspect of this video is that the giraffe is seen swimming in a pool, which is not a common sight. The giraffe is also seen jumping off a diving board and swimming underwater, which adds to the uniqueness of the video.

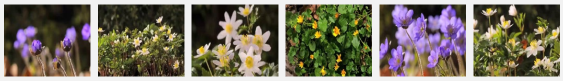

[Input Instruction] Can you write a short poem inspired from the video.

Sure, here's a short poem inspired by the video:
The flowers bloom, a gentle grace,
Their petals soft, their colors trace.
Their beauty, a sight to behold,
A moment of peace, a moment to hold.
Their colors, a symphony of hues,
A celebration of life, and all it can do.
Their beauty, a reminder to cherish,
The simple things, that bring us happiness.
So let us take a moment to appreciate,
The beauty of flowers, and all they can create.

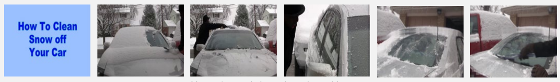

[Input Instruction] Describe the video in detail.

The video starts with a car covered in snow, and a person is seen using a scraper to remove the snow from the car's windows. The person is seen scraping the snow off the windshield and the side windows of the car. The person continues to scrape the snow off the car, making sure that all the snow is removed. The video then shows the person wiping the snow off the car's windshield and side windows. The person is seen using a cloth to wipe the snow off the car's windows, making sure that the car is completely clean. The video ends with the person finishing the job and the car being shown off. Overall, the video shows a person removing snow from a car's windows and windshield, and then wiping the snow off the car's windows to make sure it is completely clean.

[Input Instruction] Describe the video in detail.

In the video, we see a man walking down a track while holding a javelin. He then runs down the track and throws the javelin. The video then shows the man walking back to the starting point, and we see the javelin landing on the ground. The man then walks away from the camera. From the video, we can see that the man is a javelin thrower, and he is practicing his throws. The track appears to be well-maintained, and the surroundings seem to be quiet and peaceful. The man's form and technique are impressive, and it is clear that he has experience in the sport. Overall, the video provides a glimpse into the world of javelin throwing and the dedication and skill required to excel in the sport.

Figure 9: Samples of Video-LLaVA in video understanding.

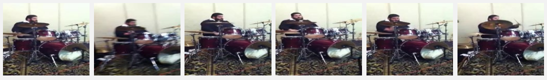

[Input Instruction] Describe the activity in the video.

The video shows a man playing the drums in a room. He is seen playing the drums with his hands and sticks, and he continues to play while looking off into the distance.

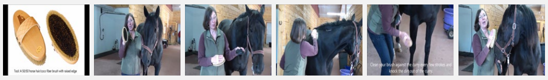

[Input Instruction] Briefly describe the video.

The video features a woman grooming a black horse in a stable. She brushes the horse's hair and cleans its hooves, and the horse is seen standing calmly throughout the process. The video also includes shots of the woman speaking to the camera and the horse.

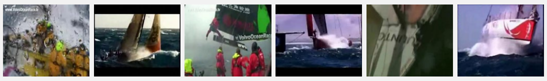

[Input Instruction] What is the main challenge faced by the people on the boat?

The main challenge faced by the people on the boat is the rough sea conditions. They are seen struggling to stay upright and maintain their balance as the boat sways back and forth.

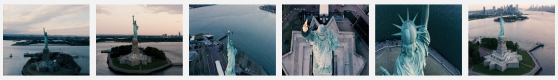

[Input Instruction] Where is this video taken from? What place/landmark is shown in the video?

The video is taken from the top of the Statue of Liberty, which is a famous landmark in New York City. The statue is shown from different angles, including from the water and from the top of the statue itself.

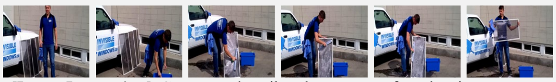

[Input Instruction] Can you describe the process for cleaning a screen window as demonstrated in the video?

Sure! The man in the video demonstrates how to clean a screen window by first wiping it down with a rag. He then applies a cleaning solution to the screen and wipes it down again. Finally, he shows how to dry the screen with a towel.

Figure 10: Samples of Video-LLaVA in video understanding.